RESEARCH ARTICLE

Experimental and mathematical evidence that thrombin-binding aptamers form a 1 aptamer:2 protein complex

Kepler S Mears[1], Daniel L Markus[1], Oluwadamilare Ogunjimi[1] and Rebecca J Whelan[1,2,*]

[1]Department of Chemistry and Biochemistry, Oberlin College, USA

[2]Department of Chemistry and Biochemistry, University of Notre Dame, USA

***Correspondence to:** Rebecca Whelan, Email: rwhelan1@nd.edu, Tel: +574-631-1853, Fax: 574-631-6652

Received: 07 September 2018 | **Revised:** 04 October 2018 | **Accepted:** 07 October 2018 | **Published:** 10 October 2018

ABSTRACT

The thrombin-binding 15mer and 29mer ssDNA aptamers are a widely used model system. Despite their ubiquity, controversies persist regarding the nature of the aptamer-protein interactions. Reported affinities vary widely; the role of metal ions in binding is unclear; the structure of the complex is contested. We interrogated the effects of instrument, buffer, and mathematical model on apparent affinities of thrombin aptamers for their target. Instrumental method had a pronounced effect on affinity constants for the 15mer and marginal effect the apparent affinity of the 29mer. Buffer composition and ionic environment did not have significant effects. Affinity probe capillary electrophoresis experiments revealed distinct peaks from samples of 29mer aptamer and thrombin, supporting the model of a 1 aptamer:2 protein complex. Fits to high quality data with five mathematical models further support this stoichiometry, as the binding of both aptamers was best described by the Hill equation with Hill coefficients > 1. Our results indicate that the instrumental method and mathematical model influence apparent affinity of thrombin aptamers and that both aptamers bind thrombin in a 1 aptamer: 2 protein stoichiometry through an induced fit mechanism.

KEYWORDS: Thrombin, DNA aptamers, thrombin-binding aptamers, affinity assays, mathematical model, Hill equation

INTRODUCTION

Aptamers are short single-stranded oligonucleotides selected to bind targets with high affinity and specificity. Aptamers are isolated through Systematic Evolution of Ligands by Exponential Enrichment (SELEX) (Ellington and Szostak, 1990; Tuerk and Gold, 1990) where ~10^{15} randomized oligonucleotides are incubated with a target; those that bind are isolated and amplified. The process is repeated with increasing selective pressure until high affinity oligonucleotides are selected. Aptamers have been selected for various targets including nucleotides (Huizenga and Szostak, 1995), small molecules (Stojanovic et al, 2001), proteins (Keefe et al, 2010), and cells (Meyer et al, 2011).

DNA aptamers selected to recognize proteins are an alternative to antibodies (Ng et al, 2006; Mairal et al, 2008; Bouchard et al, 2010). Many protein-specific DNA aptamers have affinities comparable to antibodies while possessing desirable properties such as permanent negative charge, small molecular weight, low cost of bulk synthesis, and relatively facile chemical modification enabling immobilization and/or detection (Mairal et

al, 2008). These advantages make aptamers desirable for analytical applications such as diagnostics and protein quantification.

Two ssDNA aptamers that bind thrombin, a 15mer (Bock et al, 1992) and a 29mer (Tasset et al, 1997), are the most widely used model system for aptamer-based protein detection. According to a Web of Knowledge search (accessed 6/2018), roughly 10% of all published reports on DNA aptamers involve one of these aptamers. The 15mer is a two G-quadruplex stack and the 29mer contains a similar G-quadruplex stack with an additional duplex (Macaya et al, 1993; Krauss et al, 2013). The aptamers reportedly bind different positively charged exosites on thrombin (Tasset et al, 1997; Deng et al, 2014); the 15mer targets the fibrinogen-binding site through electrostatic interactions, and the 29mer targets the heparin-binding site through hydrophobic interactions of the duplex (Lin et al, 2011). The 29mer has been reported to bind with higher affinity (Tasset et al, 1997; Deng et al, 2014).

Despite common use of the thrombin-binding aptamers, a wide range of binding constants describing the interaction of these aptamers with thrombin appear in the literature (Deng et al, 2014). The role of metal ions in binding has also been contested (Macaya et al, 1993; Kankia and Marky, 2001; Huang et al, 2004; Li et al, 2008). Table 1 summarizes the binding constants, buffers, and instrumental methods that have been used to study the thrombin aptamers. The reported values of K_d range two orders of magnitude for the 15mer and four orders of magnitude for the 29mer. Different instrumentation and buffer composition conditions are possible causes of discrepancy (Buchanan et al, 2003), but have yet to be rigorously interrogated. It is unclear whether the variation results from differences in analytical methods, ionic environment, or other factors.

The structure of the aptamer-thrombin complex has also been debated. Only a few mathematical models are routinely used to analyze aptamer-target binding data (Jing and Bowser, 2011). Most investigators model the aptamer-thrombin complex as the binding of 1 aptamer to 1 thrombin with thrombin's heparin or fibrinogen exosites interacting with the 15mer or 29mer respectively (Wu et al, 1992; Tasset et al, 1997; Nallagatla et al, 2009; Krauss et al, 2011; Deng et al, 2014). However, a reported crystal structure shows a 1 aptamer:2 protein complex with one 15mer molecule sandwiched between two thrombin molecules, interacting with both the heparin and fibrinogen sites (Padmanabhan et al, 1993; Padmanabhan and Tulinsky, 1996). 1 aptamer:2 protein binding is supported by evidence from isothermal titration calorimetry (Pagano et al, 2008) and optical thermophoresis experiments (Baaske et al, 2010). Due to the structural similarities between the 15mer and the 29mer it is plausible that the 29mer also forms a 1 aptamer:2 protein complex. Evidence of 1 aptamer:2 protein complex for the 15mer-thrombin complex has largely been ignored or interpreted as an artifact of instrumentation and experimental conditions (Nallagatla et al, 2009; Krauss et al, 2011). Because complex

stoichiometry determines the appropriate mathematical treatment of data, incorrect characterization of binding mechanism results in inaccurate affinity constants.

Using two instrumental methods—affinity probe capillary electrophoresis (APCE) and fluorescence anisotropy (FA)—six buffer environments, and five mathematical models, we studied the effects of these variables on the apparent affinity of the thrombin-binding aptamers for their target. In APCE studies, we also explored the effect of sample migration through the non-cooled capillary inlet on apparent affinity. It has been demonstrated that allowing aptamer-complexes to traverse a non-cooled capillary inlet lowers apparent affinity (Musheev et al, 2010). This effect has yet to be confirmed on a model such as the thrombin aptamers.

MATERIALS AND METHODS

Reagents

5' Texas Red and FAM labeled 15mer (5'-GGT TGG TGT GGT TGG-3') and 29mer (5'-AGT CCG TGG TAG GGC AGG TTG GGG TGA-3') thrombin-binding aptamers were purchased from IDT (Coralville, IA). Aptamers were reconstituted to 100µM in TE buffer (10mM Tris, 0.1mM EDTA, pH 8.0) following instructions provided by the vendor. The volume of diluent used for reconstitution was determined using optical density measurements and an extinction coefficient calculated specifically for the nucleotide sequence. Reconstituted aptamers were stored at -20°C. Lyophilized thrombin from human plasma (Sigma) was reconstituted to 1000U/ml (diluent was a solution of 1mg BSA/ml water), distributed into aliquots, flash frozen on liquid nitrogen, and stored at -80°C. TG (192mM Tris, 25mM glycine, pH 8.3) and PBS (0.1M sodium phosphate, 0.15M NaCl, pH 7.2) came from Thermo Scientific, KH_2PO_4 from Mallinckrodt, $MgCl_2$ from Sigma, and rhodamine 110 from Fluka. TGK was prepared from TG by the addition of KH_2PO_4 to a concentration of 5mM. TGKM was prepared from TGK with the addition of $MgCl_2$ to a final concentration of 5mM. TGM was prepared by adding $MgCl_2$ to TG to a concentration of 5mM. Buffers were prepared using 18.2MΩ cm water at 25°C and pH adjusted with NaOH.

Capillary electrophoresis with laser-induced fluorescence

All electrophoresis experiments were performed using unmodified fused silica capillaries (50cm length, 50µm inner diameter, 360µm outer diameter; Polymicro Technologies, Inc., Phoenix, AZ) in a Beckman Coulter P/ACE MDQ system (Fullerton, CA) with laser induced fluorescence (LIF) detection. Separations were performed in both normal and reverse polarity, allowing two possible lengths from injection to detector: 39.5cm and 10.5cm, respectively. Electrophoresis buffer was TGK.

A 488nm Ar^+ laser (Beckman Coulter) and a 594nm HeNe laser (Research Electro-Optics, Inc., Boulder, CO) with fluorescence detected at 520nm and 620nm respectively were used for LIF detection. HeNe laser output was coupled to a single pass multimode fiber optic via a SMA coupler (Thorlabs, Newton, NJ). An Advantest optical power meter was used to measure laser intensity. A 594nm bandpass filter (Edmund Optics, Barrington, NJ) and adjustable iris (Thor Labs) were placed between the laser head and fiber coupler. An additional 594nm notch filter (Semrock Inc., Buffalo, NY) was installed internally to the instrument. Conditioning of HeNe laser output was crucial to obtaining low signal-to-noise by removing non-coherent radiation.

Affinity probe capillary electrophoresis

2.5µM aptamer stocks were prepared in TE. Stocks were diluted in 4.5x volume TGK, heated to 95°C for 3min and cooled to 4°C. Samples contained 20nM rhodamine 110 as an internal standard, 0.2mg BSA/ml buffer, 75nM aptamer, varied concentrations of thrombin (from 0-900nM), and TGK to bring samples to volume. Samples were incubated at 25°C in the dark for 1hr before analysis. A Mastercycler Personal (Eppendorf, Hamburg, Germany) was used for melting and incubation.

To eliminate the effects of the non-cooled capillary inlet (NCI), a pressure separation was incorporated before applying high voltage. Solving the Poiseuille equation (online at CE Expert Lite, Sciex) determined that for a 1.2cm inlet, application of 0.5psi for 1.17min was sufficient to bypass the NCI. Samples were incubated until they were run on the CE. A conditioning rinse (0.5min each NaOH, MilliQ and TGK; 20psi) was performed prior to analysis.

A metric associated with decreased peak height, equation 1, served as a proxy for complex formation, where I_0 is the height of the free aptamer peak in the absence of protein and I is the free aptamer peak height at a given protein concentration. Peak height was normalized to the rhodamine 110 peak height.

$$Fraction\ bound = f_b = \frac{(I_0\text{-}I)}{I_0} \quad (1)$$

Theoretically, f_b ranges from 0 to 1 with saturated binding occurring at $f_b = 1$. Practically, binding can saturate at $f_b < 1$, which necessitates the inclusion of a fit parameter (B_{max}) in affinity models.

Fluorescence anisotropy

Fluorescence anisotropy experiments were performed on a SpectraMax M5 plate reader with excitation at 585nm, emission at 635nm, and wavelength cut-off at 610nm. Samples were prepared as for APCE, without

rhodamine 110. Texas Red labeled aptamers were used (Gokulrangan et al, 2005). Samples were loaded in duplicate, 100µl/well, in a 96 well plate, covered with Parafilm, and incubated in the plate reader at 25°C for 1hr prior to analysis.

For APCE/FA hybrid assays, samples were prepared as for APCE experiments with Texas Red labeled aptamers. After sample preparation, two aliquots of sample were distributed into a 96 well plate and incubated as for FA analysis. The remaining samples were incubated for APCE experiments.

Affinity models

All models were fit to isotherm data using non-linear least squares fitting with Igor Pro (Wavemetrics). Derivations are in Supporting Information. The most widely used model for fitting affinity data is the square hyperbola which models a 1:1 aptamer protein association (equation 2):

$$f_b = \frac{B_{max}[P]_t}{K_d + [P]_t} \quad (2)$$

Where $[P]_t$ is total protein concentration, K_d the dissociation constant and B_{max} a fit parameter. K_d can be interpreted as the concentration of protein resulting in half maximum binding of aptamer. The square hyperbola is simple and can be easily linearized, but to be applicable the total concentration of aptamer must be significantly less than the total concentration of protein.

If the concentration of aptamer is not significantly less than the concentration of protein, equation 2 must be expanded. The resulting model (equation 3) depends on both aptamer and protein concentrations:

$$f_b = \frac{B_{max}\left(([A]_t + [P]_t + K_d) - \sqrt{([A]_t + [P]_t + K_d)^2 - 4[A]_t[P]_t}\right)}{2[A]_t} \quad (3)$$

For the case of 1 aptamer: 2 protein associations the most straightforward model is a two independent non-interacting sites model (equation 4). Equation 4 is the addition of two square hyperbolas and returns a value of K_d and B_{max} for each binding site.

$$f_b = \frac{B_{max1}[P]}{K_{d1} + [P]} + \frac{B_{max2}[P]}{K_{d2} + [P]} \quad (4)$$

Alternatively, a complex can form through a stepwise association (equation 5), involving the formation of first a 1:1 complex then a 1 aptamer:2 protein complex.

$$f_b = \frac{B_{max}(K_{d2}[P] + [P]^2)}{K_{d1}K_{d2} + K_{d2}[P] + [P]^2} \quad (5)$$

The Hill equation (equation 6) provides a general way to model higher-order stoichiometries. The Hill equation returns the Hill coefficient "n" and K_A rather than K_d. K_A has the same units as K_d for 1:1 complex stoichiometry and represents the concentration of protein at half maximum binding. Empirically "n" refers to the number of ligands but practically is referred to as the cooperativity and represents the strength of interaction between multiple binding sites. A value of $n > 1$ indicates positive cooperative binding and multiple binding sites while $n < 1$ is negatively cooperative. When $n = 1$ the Hill equation reduces to the square hyperbola (equation 2) and $K_A = K_d$.

$$f_b = \frac{B_{max}[P]^n}{{K_A}^n + [P]^n} \quad (6)$$

The Hill equation was determined to best model both the 15mer and 29mer, and was used to determine apparent affinity for all other experiments with the quantifying metric of affinity being K_A.

Quantifying model fit

Two metrics are used to compare affinity models: relative standard deviation of binding constants (RSD) and root mean squared of residuals (RMS). The RSD of fit coefficients, and in turn the binding constant, is determined by Igor Pro during fitting using the Levenberg-Marquardt algorithm. The RMS of residuals is calculated after subtracting the fit from the raw data. A low RSD value indicates that the fit coefficients uniquely describing the raw data; low RMS of residuals indicates that the resulting coefficients precisely model the raw data. Both RSD and RMS are required as it is possible to have high value of RSD with low RMS and vice versa. Together RSD and RMS are used to evaluate the quality of a model fit.

RESULTS AND DISCUSSION

Effects of buffer composition

The role of buffer composition, specifically cations, on the binding of the thrombin aptamers is unclear. K^+ is known to coordinate G-quadruplexes in DNA whereas Mg^{2+} stabilizes duplexes (Hardin et al, 1992; Robinson et

al, 2000). Consequently, researchers have found that K^+ stabilizes the G-quadruplex of folded 15mer (Kankia and Marky, 2001; Huang et al, 2004; Kraus et al, 2012) and Mg^{2+} stabilizes the A-form duplex in folded 29mer (Lin et al, 2011). Conversely, Mg^{2+} was found to have little effect on 15mer structure and K^+ had little to no effect on the 29mer duplex stability (Kankia and Marky, 2001; Huang et al, 2004). Despite the evidence that K^+ stabilizes G-quadruplexes in the thrombin aptamers, crystal structures of 15mer bound to thrombin found no evidence of K^+ in the quadruplex (Padmanabhan et al, 1993; Padmanabhan and Tulinsky, 1996). Other publications demonstrate that cations are not necessary for proper folding of either aptamer (Li et al, 2008; Song et al, 2009).

To clarify the role of cations on binding of the thrombin aptamers, we characterized aptamer-thrombin binding using FA experiments in five buffers. TG, TGK, TGM and TGKM were used to evaluate the effect of K^+ and Mg^{2+} on apparent affinity; PBS was used to evaluate high ionic strength. The results are summarized in Table 2 and indicate that binding of these aptamers to their targets is not significantly affected by buffer system. TGK provides the worst apparent environment for binding, with K_A = 51.8nM, roughly twice that of other systems; all other buffers perform comparably. This observation is contrary to previous reports that stabilization of the 15mer G-quadruplex is essential for binding (Kraus et al, 2012). TGM provides the best binding environment for the 29mer with K_A = 30.8nM, consistent with formation of a folded duplex during binding to thrombin, although the effect is marginal (Lin et al, 2011). The observed weak correlation between cation and affinity suggests that increased structure of folded 15mer and 29mer in the presence of cations does not increase binding affinity. If K^+ and Mg^{2+} ions affect aptamer structure, as previously reported, that structure does not influence binding affinity. Lack of structural requirements indicates the aptamers bind through an induced fit, rather than a lock-and-key, mechanism.

Instrumental effects

To our knowledge there has been no systematic comparison of instrumental methods on the binding of the thrombin aptamers. To examine the effects of instrumentation, APCE and FA assays were performed on 5'-Texas-Red-labeled thrombin aptamers. Theoretically, characterizing aptamer-protein binding in identical samples using different instrumental methods should result in the same affinity constants, but we observe differences, as shown in Figure 1 and Table 3.

We hypothesized that APCE would consistently yield higher values of K_A (lower apparent affinity) as APCE is a non-equilibrium technique. This was observed only for the 15mer. The 29mer displayed slightly greater affinity when characterized by APCE than FA, although the effect is not statistically significant. The consistency of affinity values for the 29mer across methods could be explained by its formation of a more stable complex

with lower dissociation rate constant (Hianik et al, 2005). Though the 15mer with a Texas Red label has consistently greater affinity when assayed by FA than the comparably labeled 29mer, it may have a faster off rate and degrade faster during APCE, resulting in a lower apparent affinity. The more stable 29mer would have similar affinity for both APCE and FA as the complex would not dissociate during separation. Surface plasmon resonance studies on label-free thrombin aptamers found the 15mer has a slower off rate than the 29mer (Lin et al, 2011). Because the binding kinetics of Texas Red labeled aptamers have not been characterized, we cannot directly compare the results of SPR experiments and those reported here. The presence of the fluorophore seems to alter the dissociation rate constant for the 15mer; this effect must be further investigated.

Non-cooled capillary inlet

The Krylov group demonstrated that the non-cooled capillary inlet (NCI) of commercially available CE instruments can introduce systematic error in affinity determination (Musheev et al, 2010). Heating in the NCI under applied high voltage promotes complex dissociation, underestimating affinity. A NCI-dependent effect on affinity has yet to be demonstrated on a model system such as thrombin or with canonical data analysis. An earlier report similarly found increased field strength degrades aptamer-protein complex using uninsulated capillaries on a home-built instrument, but dismissed the possibility of the degradation being caused by heat (German et al, 2003).

APCE experiments were performed with and without the NCI. Pressure was applied to push sample past the NCI. Isotherms were fit with the Hill equation; resulting values of K_A are summarized in Table 4. Including the NCI during separations results in a statistically significant higher K_A ($p < 0.001$) for both aptamers, confirming previously published results (Musheev et al, 2010). Field strength was consistent, whether the NCI was included or excluded, isolating the effect to the NCI. As the NCI artificially lowers K_A, it was excluded for all other APCE experiments.

1 Aptamer: 2 Protein Complex Observed in Electropherograms

In APCE electropherograms for the 29mer the free aptamer peak and two complex peaks are clearly observed, as seen in Figure 2. The peaks were confirmed to be complexes via competitive binding experiments with unlabeled 29mer (data not shown). The free aptamer peak is not completely eliminated when saturated binding is reached. The remaining fluorescence is likely due to a fluorescent byproduct or mis-folded aptamer and does not interfere with analysis.

The two complex peaks likely correspond to two different stoichiometric ratios of complex i.e. 1 aptamer:1 protein and 1 aptamer:2 protein complexes. The earlier-eluting complex (labeled Complex 1 in Figure 3) is more pronounced at lower thrombin concentrations and decreases with increasing thrombin concentration, while the later-eluting Complex 2 increases. The shift in peak profile suggests that the complex is 1 aptamer:2 protein rather than 2 aptamer:1 protein. If the complex had been 2 aptamer:1 protein, increasing protein concentration would favor the 1:1 complex and degrade 2 aptamer:1 protein complex, resulting in a single complex peak. The shift also supports model of stepwise complex formation. If the complex resulted from independent binding sites, the two complexes would increase together with increasing thrombin.

A complex peak is observed for the 15mer and confirmed with a competitive experiment (data not shown). A contaminant/misfolded peak is also observed. The 15mer contaminant peak is not diminished with increased thrombin while the free aptamer peak is completely diminished. The separation of 15mer folded and mis-folded aptamer has been reported previously (Huang et al, 2004).

Model effects on the measured affinity

APCE data were collected for both aptamers. Isotherms generated from affinity data were analyzed using 5 affinity models. Example fits for the 29mer are in Figure 3. Based on these fits, binding constants, RSD of binding constant and RMS of residuals where applicable were calculated. The resulting values are in Table 5.

The 1 aptamer:2 protein stepwise model (equation 6) provides the lowest RMS of residuals for both aptamers; however, it returns a poor RSD compared to the square hyperbola. The stepwise model most accurately describes the thrombin aptamers' binding, but due to a large RSD is poor at differentiating changes in affinity. A large RSD indicates a large fit scape in which possible combinations of fit coefficients closely model the data and the algorithm has difficulty distinguishing two or more coefficients. Covariance matrices for the stepwise model were computed for both sets of data, the covariance between K_{d1} and K_{d2} was greater in magnitude than 0.997 (data not shown) for both aptamers indicating that K_{d1} and K_{d2} are the source of the large RSD of coefficient and that this is inherent to the model, limiting the utility of the stepwise model since the differences between K_{d1} and K_{d2} are hard to determine. The independent site model (equation 5) provides the worst fit in terms of both RSD and RMS, indicating that 2 aptamer:1 protein complex is not formed through independent interactions. The Hill equation provides the lowest RSD and a low RMS compared to the square hyperbola. While the Hill equation does not model affinity data most precisely, it is considered to have the best fit based on the balance of low RSD and RMS. For both aptamers the Hill equation returns $n > 1$, indicating positive cooperativity for both aptamers, as is also evident in the sigmoid shape of the curve in Figure 3.

CONCLUSION

Cations were not observed to have a significant effect on the affinity of the thrombin aptamers. This result indicates the aptamers tolerate a variety of environments, and that the secondary and tertiary structure is either independent of ions or that ions are not important for binding. As structural ions are not important for binding it is likely that the aptamers bind thrombin through induced fit, which has been previously suggested for the 15mer (Baldrich and O'Sullivan 2005). The effect of instrumental method is different for the two aptamers. There is little to no effect on the 29mer whereas APCE resulted in a lower apparent affinity for the 15mer, likely due to a fast off rate. The NCI of the capillary electrophoresis instrument lowers apparent affinity for both aptamers, consistent with previous reports (Musheev et al, 2010).

The applied mathematical model has significant effect on apparent affinity. Both the 15mer and 29mer are fit most precisely by a 1 aptamer:2 protein model and overall best modeled by the Hill Equation. A 1 aptamer:2 protein complex with no K^+ ions has been demonstrated previously with the 15mer binding both exosites (Padmanabhan et al, 1993; Padmanabhan and Tulinsky, 1996). Given structural similarities the 29mer likely behaves similarly. A 1 aptamer:2 protein complex was observed for the 29mer in CE electropherograms. Our results suggest that both the 15mer and 29mer bind thrombin via a 1 aptamer:2 protein complex that is formed stepwise and cooperatively through induced fit. This stoichiometry should be considered when designing experiments. We recommend that the Hill equation be used when analyzing 15mer and 29mer affinity data. A low RSD is critical for measuring differences in protein-aptamer affinity and is advantageous for the affinity of aptamer in response to different conditions to be interrogated. We suggest that observed affinity depends on instrumental methods and mathematical models used and that the 29mer does not strictly have higher affinity for thrombin than the 15mer. Finally, for experiments that determine binding affinity of novel aptamers, we advocate that affinities not be compared to literature values for the 15mer and 29mer determined with different methodology. Because these literature values vary widely and differ according to instrumentation and mathematical modeling, we advocate that labs should independently determine affinities for the 15mer and 29mer if they are to be compared to affinities of novel aptamers.

ACKNOWLEDGEMENTS

The project described was supported by Grant Number R15CA161970 from the National Cancer Institute. The content is solely the responsibility of the authors and does not necessarily represent the official views of the National Cancer Institute or the National Institutes of Health. Financial support from a Henry Dreyfus Teacher

Scholar Award (to RJW) is acknowledged. We thank Bill Mohler for instrument support and Professor Jason Stalnaker for valuable consultation.

COMPETING INTERESTS

None declared.

ABBREVIATIONS

APCE: affinity probe capillary electrophoresis

FA: fluorescence anisotropy

K_A: binding metric returned by the Hill equation

K_d: dissociation constant

NCI: non-cooled capillary inlet

PBS: phosphate buffered saline

RSD: relative standard deviation

RMS: root means squared of the residuals

TE: Tris EDTA buffer

TG: Tris glycine buffer

TGK: Tris glycine buffer with potassium

TGKM: Tris glycine buffer with potassium and magnesium

TGM: Tris glycine buffer with magnesium

REFERENCES

Baaske P, Wienken CJ, Reineck P, Guhn S and Braun D. 2010. Optical Thermophoresis for Quantifying the Buffer Dependence on Aptamer Binding. Angew Chem Int Ed, 49, 2238-2241.

Baldrich E, O'Sullivan CK. 2005. Ability of thrombin to act as molecular chaperone, inducing formation of a quadruplex structure of thrombin-binding aptamer. Anal Biochem, 1, 194-197.

Berezovski M, Nutiu R, Li Y and Krylov SN. 2003. Affinity Analysis of a Protein-Aptamer Complex Using Nonequilibrium Capillary Electrophoresis of Equilibrium Mixtures. Anal Chem, 75, 1382-1366.

Bock LC, Griffin LC, Latham JA, Vermaas EH and Toole JJ. 1992. Selection of single-stranded DNA molecules that bind and inhibit human thrombin. Nature, 355, 564-566.

Bouchard PR, Hutabarat RM and Thompson KM. 2010. Discovery and Development of Therapeutic Aptamers. Annu Rev Pharmacol Toxicol, 50, 237-57.

Buchanan DD, Jameson EE, Perlette J, Malik A and Kennedy RT. 2003. Effects of buffer, electric field, and separation time on detection of aptamer-ligand complexes for affinity probe capillary electrophoresis. Electrophoresis, 24, 1375-1382.

Deng B, Lin Y, Wang C et al. 2014. Aptamer binding assays for proteins: the thrombin example—a review. Anal Chim Acta, 837, 1-15.

Ellington AD and Szostak JW. 1990. In vitro selection of RNA molecules that bind specific ligands. Nature, 346, 818-822.

German I, Buchanan DD and Kennedy RT. 1998. Aptamers as ligands in affinity probe capillary electrophoresis. Anal Chem, 70, 4540-4545.

Gokulrangan G, Unruh JR, Holub DF, Ingram B, Johnson CK and Wilson GS. 2005. DNA aptamer-based bioanalysis of IgE by fluorescence anisotropy. Anal Chem, 77, 1963-1970.

Gong M, Nikcevic I, Wehmeyer KR, Limbach PA and Heineman WR. 2008. Protein-Aptamer Binding Studies Using Microchip Affinity Capillary Electrophoresis. Electrophoresis, 29, 1415-1422.

Hardin CC, Watson T, Corregan M and Bailey C. 1992. Cation-dependent transition between the quadruplex and Watson-Crick hairpin forms of d(CGCG$_3$GCG). Biochemistry, 31, 833-841.

Hianik T, Ostatná V, Sonlajtnerova M and Grman I. 2007. Influence of ionic strength, pH and aptamer configuration for binding affinity to thrombin. Bioelectrochemistry, 70, 127-133.

Huang C, Cao Z, Chang H and Tan W. 2004. Protein-protein interaction studies based on molecular aptamers by affinity capillary electrophoresis. Anal Chem, 76, 6973-6981.

Huizenga DE and Szostak JW. 1995. A DNA aptamer that binds adenosine and ATP. Biochemistry, 34, 656-665.

Jing M, Bowser MT. 2011. Methods for measuring aptamer-protein equilibria: A review. Analytica Chimica Acta, 686, 9-18.

Kankia BI and Marky LA. 2001. Folding of the thrombin aptamer into a G-quadruplex with Sr^{2+}: stability, heat, and hydration. J Am Chem Soc, 123, 10799-10804.

Keefe AD, Pai S and Ellington A. 2010. Aptamers as therapeutics. Nat Rev Drug Discov, 9, 537-550.

Krauss IR, Merlino A, Giancola C, Randazza A, Mazzarella L and Sica F. 2011. Thrombin-aptamer recognition: a revealed ambiguity. Nucl Acids Res, 39, 7858-7867.

Krauss IR, Pica A, Merlino A, Mazzarella L and Sica F. 2013. Duplex-quadruplex motifs in a peculiar structural organization cooperatively contribute to thrombin binding of a DNA aptamer. Acta Cryst D, 69, 2403-2411.

Li H-Y, Deng Q-P, Zhang D-W, Zhou Y-L and Zhang X-X. 2010. Chemiluminescently labeled aptamers as the affinity probe for interaction analysis by capillary electrophoresis. Electrophoresis, 31, 2452-2460.

Li Y, Guo L, Zhang F, Zhang Z, Tang J, Xie J. 2008. High-sensitive determination of human ∝-thrombin by its 29-mer aptamer in affinity probe capillary electrophoresis. Electrophoresis, 29, 2570-2577.

Lin P, Chen R, Lee C, Chang Y, Chen C and Chen W. 2011. Studies of the binding mechanism between aptamers and thrombin by circular dichroism, surface plasmon resonance and isothermal titration calorimetry. Colloids Surf B Biointerfaces, 88, 552-558.

Macaya R, Schultze P, Smith FW, Roe JA and Feigon J. 1993. Thrombin-binding DNA aptamer forms a unimolecular quadruplex structure in solution. Proc Natl Acad Sci USA, 90, 3745-3749.

Mairal T, Özalp VC, Sánchez PL, Mir M, Katakis and O'Sullivan CK. 2008. Aptamers: molecular tools for analytical applications. Anal Bioanal Chem, 390, 989-1007.

Meyer C, Hahn U and Rentmeister A. 2011. Cell-specific aptamers as emerging therapeutics. J Nucleic Acids, ID904750, 1-18.

Musheev MU, Filiptsev Y, Krylov SN. 2010. Noncooled capillary inlet: a source of systematic errors in capillary-electrophoresis-based affinity analyses. Anal Chem, 82, 8637-8641.

Nallagatla SR, Heuberger B, Haque A and Switzer C. 2009. Combinatorial Synthesis of Thrombin-Binding Aptamers Containing iso-Guanine. J Comb Chem, 11, 364-369.

Ng EWM, Shima DT, Calias P, Cunningham ET, Jr., Guyer DR and Adamis AP. 2006. Pegaptanib, a targeted anti-VEGF aptamer for ocular vascular disease. Nature Rev, 5, 123-132.

Padmanabhan K, Padmanabhan KP, Ferrara JD, Sadler JE and Tulinsky A. 1993. The structure of ∝-thrombin inhibited by a 15-mer single-stranded DNA aptamer. J Biol Chem, 268, 17651-17654.

Padmanabhan K and Tulinsky. 1996. An ambiguous structure of a DNA 15-mer thrombin complex. Acta Cryst D, 52, 272-282.

Pagano B, Martino L, Randazzo A and Giancola C. 2008. Stability and Binding Properties of a Modified Thrombin Binding Aptamer. Biophys J, 94, 562-569.

Robinson H, Gao Y, Sanishvili R, Joachimiak A and Wang AHJ. 2000. Hexahydrated magnesium ions bind in the deep major groove and at the outer mouth of A-form nucleic acid duplexes. Nucleic Acids Res, 28, 1760-1766.

Song M, Zhang Y, Li T, Wang Z, Yin J and Wang H. 2009. Highly sensitive detection of human thrombin in serum by affinity capillary electrophoresis/laser-induced fluorescence polarization using aptamers as probes. J Chrom A, 1216, 873-878.

Stojanovic MN, de Prada P and Landry DW. 2001. Aptamer-based folding fluorescent sensor for cocaine. J Am Chem Soc, 123, 4928-4931.

Tasset DM, Kubik MF and Steiner W. 1997. Oligonucleotide inhibitors of human thrombin that bind distinct epitopes. J Mol Biol, 272, 688-698.

Tuerk C and Gold L. 1990. Systematic evolution of ligands by exponential enrichment: RNA ligands to bacteriophage T4 DNA polymerase. Science, 249, 505-510.

Wu Q, Tsiang M and Sadler JE. 1992. Localization of the Single-stranded DNA Binding Site in the Thrombin Anion-binding Exosite. J Biol Chem, 267, 24406-24412.

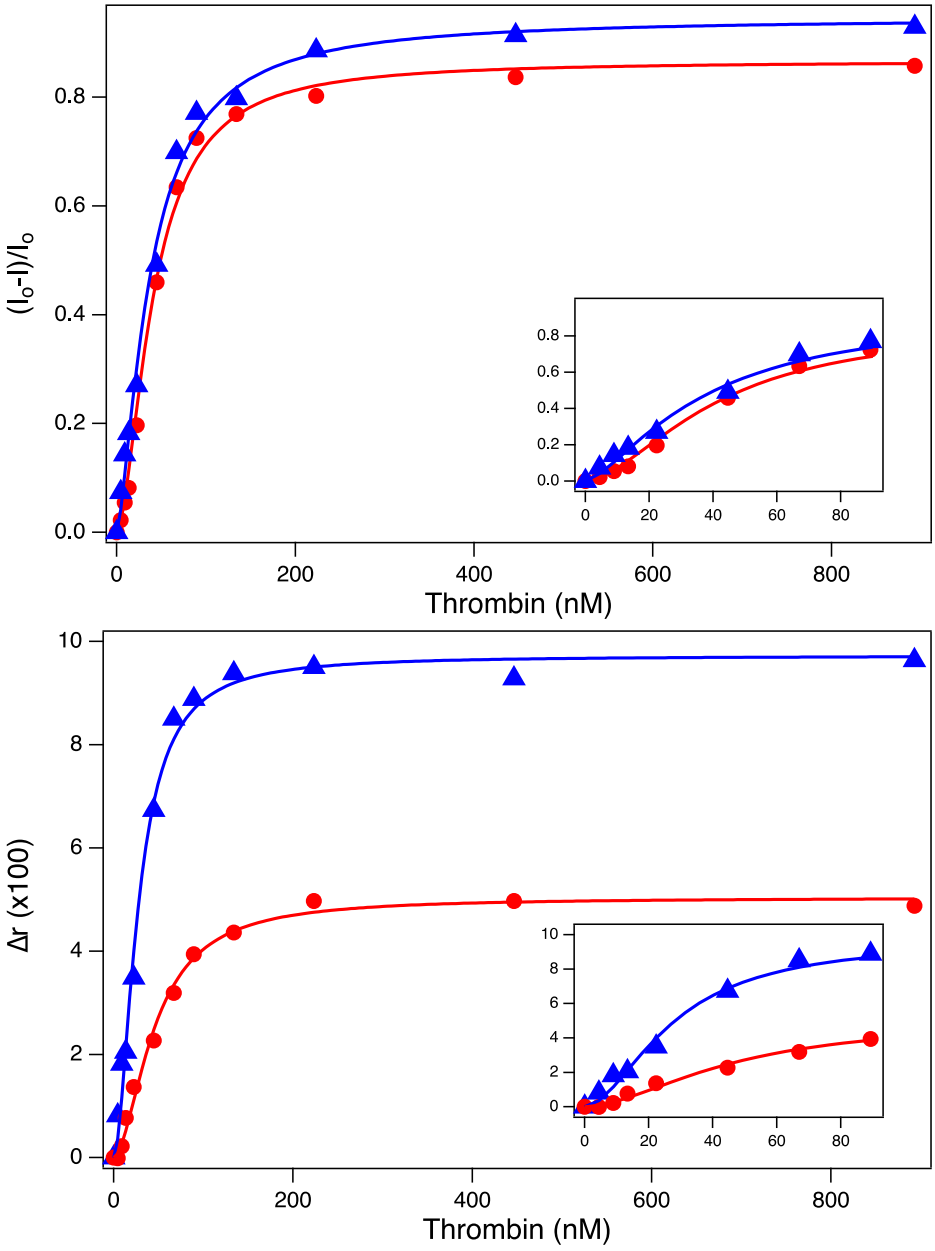

Figure 1. Isotherms generated from FA (top) and APCE (bottom) assay. The isotherms for the 15mer are in blue triangles; isotherms for the 29mer are in red circles. Insets show the low-concentration range of the isotherm.

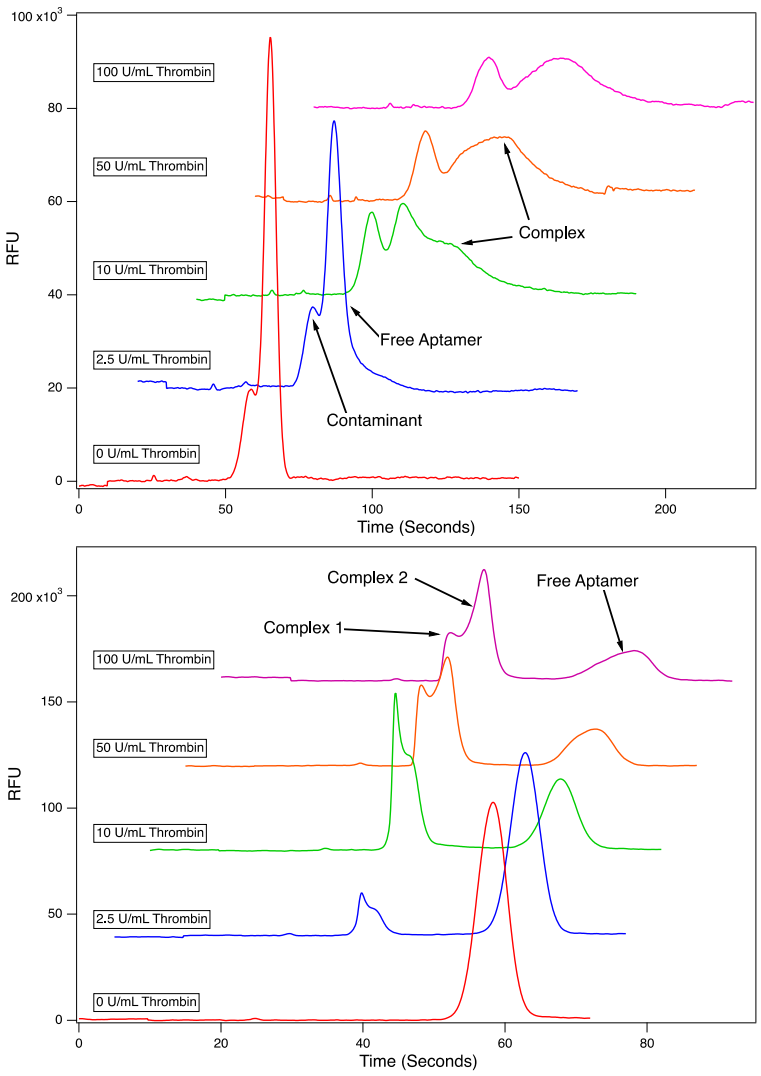

Figure 2. APCE electropherogram data for the thrombin 29mer (right) and 15mer (left). Two distinct complex peaks are seen in the 29mer electropherogram data that shift in intensity with thrombin concentration. The 15mer complex peak is observed at a different migration time, is less defined, and overlaps with the free aptamer peak.

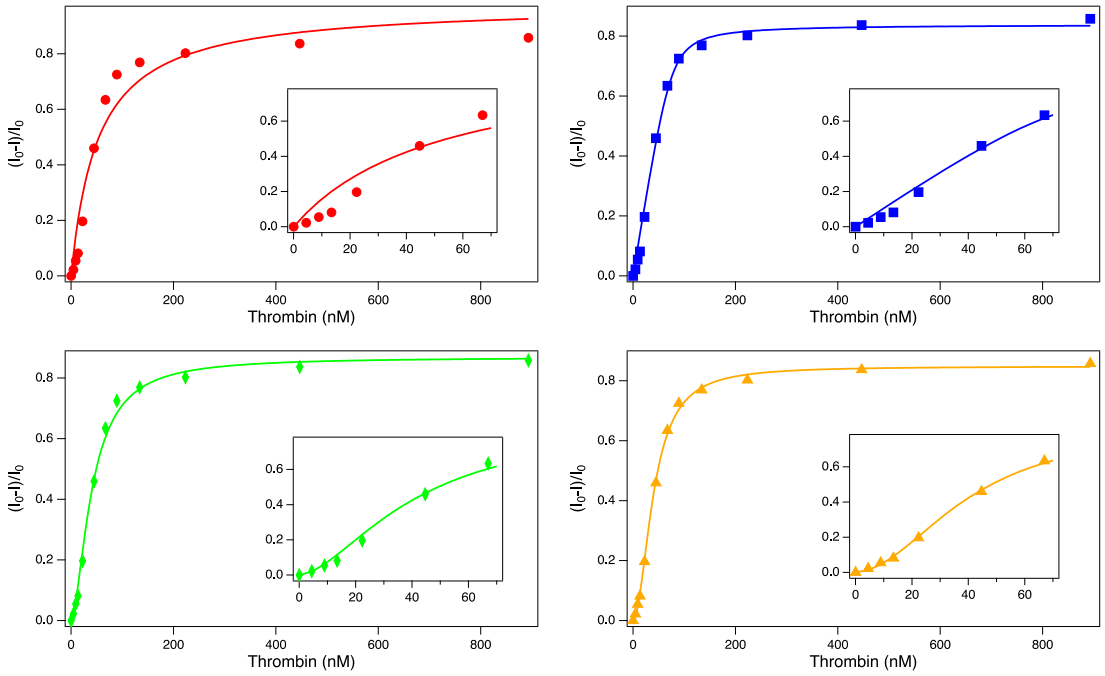

Figure 3. Model fits to 29mer APCE data. Square hyperbola (red circles, top left), expanded hyperbola (blue squares, top right), 1 aptamer:2 protein stepwise (orange triangles, bottom right) and the Hill equation (green diamonds, bottom left). Insert shows the lower concentration range where a sigmoid shape is apparent.

Table 1. Summary of the instrumental methods, buffer conditions and binding models previously used to determine binding constants of the thrombin aptamers.

Aptamer	Binding Constant	Method	Buffer Conditions	Model
15mer	EC_{50} = 25nM (Bock et al, 1992)	Nitrocellulose Filter Binding	20mM Tris-acetate, pH 7.4, 140 mM NaCl, 5mM KCl, 1mM $CaCl_2$, 1mM $MgCl_2$	N/A
	K_d = 54.911nM (Lin et al, 2011)	Surface Plasmon Resonance	10mM Tris-HCl, 5mM KCl, 1mM $MgCl_2$, 1mM $CaCl_2$, 50mM NaCl, pH 7.4	1:1 from kinetics
	K_d = 20nM (Huang et al, 2004)	Affinity Probe Capillary Electrophoresis	10mM Tris-HCl, 15mM KCl, pH 8.4	NECEEM
	K_d = 450nM (German et al, 1998)	Affinity Probe Capillary Electrophoresis	5mM Na_2HPO_4, 5mM KH_2PO_4, 2mM $MgCl_2$, pH 8.2	Simple Isotherm
	K_d = 240±16nM (Berezovski et al, 2003)	Affinity Probe Capillary Electrophoresis	20mM Tris-HCL, pH 8.3, 5mM KCl, 1mM $MgCl_2$	NECEEM
	K_d = 43nM (Gong et al, 2008)	MicroChip Affinity Capillary Electrophoresis	25mM Tris, 192mM 5mM HCl	NECEEM
	K_b = 3±1e6 M^{-1} (Pagano et al, 2008)	Isothermal Titration Calorimetry	10 mM potassium phosphate, 70 mM KCl, 0.1 mM EDTA at pH 7.0	Unspecified 1 aptamer:2 protein model
	K_d = 30±19nM (Baaske et al, 2010)	Optical Thermophoresis	20mM Tris-acetate, pH 7.4, 140 mM NaCl, 5mM KCl, 1mM $CaCl_2$, 1mM $MgCl_2$	N/A
	EC_{50} = 720±100nM (n = 2) (Baaske et al, 2010)	Optical Thermophoresis	50% serum	Hill Equation
	K_d = 94.4 ± 26.6 nM (n = 1.13) (Nallagatla et al, 2009)	Optical Thermophoresis	20 mM Tris acetate pH 7.3, 140 mM NaCl, 5mM KCl, 1 mM $MgCl_2$ and 1 mM $CaCl_2$	Single site binding curve from Origin 5 software package
20mer (modified 15mer)	K_d = 39±27nM (Hianik et al, 2007)	Cyclic Voltametry	140mM NaCl, 5mM KCl, 1mM CaCl2, 1mM MgCl2, 20mM Tris pH 7.4	1:1 from kinetics
29mer	K_d = 0.5 nM (Tasset et al, 1997)	Nitrocellulose Filter Binding	50mM Tris-HCl, pH 7.5, 100mM NaCl, 1mM $MgCl_2$	Standard competitive binding model
	K_d = 119.5nM (Lin et al, 2011)	Surface Plasmon Resonance	20mM Tris-HCl, 5mM KCl, 1mM $MgCl_2$, 1mM $CaCl_2$, 50mM NaCl, pH 7.4	1:1 from kinetics
	K_d = 31.1nM (Song et al, 2009)	Capillary Electrophoresis with Laser Induced Fluorescence Polarization	1xTG, pH 8.3, 5mM KCl	NECEEM
	K_d = 255±54nM (Li et al, 2008)	Affinity Probe Capillary Electrophoresis	2XTG, pH 8.5	Simple isotherm
	K_d = 124.0±6.9 (n = 0.81) (Li et al, 2010)	Affinity Probe Capillary Electrophoresis with Chemillumuniscent Detection	TGK 8.5 with HRP in anode vial TK with H2O2 in cathode vial TGKMg for sample prep	X, Y, double reciprocal plot
32mer (modified 29mer)	K_d = 88±53 (Hianik et al, 2007)	Cyclic Voltametry	140mM NaCl, 5mM KCl, 1mM CaCl2, 1mM MgCl2, 20mM Tris pH 7.4	1:1 reversible interaction from kinetics

Table 2. Values of K_A and Hill coefficients from FA experiments of the thrombin aptamers in different ionic environments; Tris-Glycine (TG), Tris-Glycine Potassium (TGK), Tris-Glycine Magnesium (TGM), Tris-Glycine Potassium/Magnesium (TGKM) and phosphate buffered saline (PBS). (N = 3).

Aptamer	TG	TGK	TGM	TGKM	PBS
15mer	K_A = 25.0 ± 1.5 nM n = 1.62 ± 0.16	K_A = 51.8 ± 2.9 nM n = 1.810 ± 0.090	K_A = 30.4 ± 2.6 nM n = 1.36 ± 0.11	K_A = 23.7 ± 1.1 nM n = 1.76 ± 0.13	K_A = 29.7 ± 1.1 nM n = 1.355 ± 0.047
29mer	K_A = 41.5 ± 2.4 nM n = 1.66 ± 0.10	K_A = 49.2 ± 4.4 nM n = 1.64 ± 0.15	K_A = 30.5 ± 1.8 nM n = 1.78 ± 0.11	K_A = 43.1 ± 4.2 nM n = 1.209 ± 0.080	K_A = 37.0 ± 3.6 nM n = 1.228 ± 0.083

Table 3. A comparison of APCE and FA on the apparent affinity of the thrombin aptamers via APCE+FA hybrid assay. Values of K_A and Hill coefficient for the APCE and FA portions of the hybrid assay for the 15mer and 29mer thrombin-binding aptamers. TGK was used as the assay buffer; aptamers were 5'-labeled with Texas Red.

Aptamer	APCE	FA
15mer (N = 3)	K_A = 37.0 ± 2.2 nM n = 1.450 ± 0.066	K_A = 27.3 ± 1.6 nM n = 1.80 ± 0.11
29mer (N = 5)	K_A = 40.9 ± 1.9 nM n = 1.683 ± 0.060	K_A = 45.6 ± 2.5 nM n = 1.77 ± 0.11

Table 4. The effects of the NCI on the apparent affinity of the thrombin aptamers. Values of K_A are from APCE experiments for the 15mer and 29mer with and without the NCI. For both the 15mer and 29mer, excluding the NCI results in a lower K_A i.e. higher affinity (N = 3).

Aptamer	With NCI	Without NCI
15mer Fl	K_A = 60.9 ± 5.3 nM n = 1.44 ± 0.13	K_A = 49.2 ± 1.2 nM n = 1.537 ± 0.046
29mer Fl	K_A = 39.9 ± 1.9 nM n = 1.510 ± 0.064	K_A = 32.0 ± 2.3 nM n = 1.334 ± 0.074

Table 5. Summary of models used to fit APCE data for the 15mer and 29mer and the resulting binding constants. Models were fit using nonlinear least squares on Igor Pro along and all statistical values extracted from the result of the fitting.

Model	15mer			29mer		
	Constant	RSD of Constant	RMS of residuals	Constant	RSD of Constant	RMS of residuals
Square Hyperbola	K_d = 44.6 ± 6.3 nM	14%	0.0485	K_d = 53 ± 12 nM	23%	0.0725
Expanded Square Hyperbola	K_d = 4.5 ± 1.4 nM	31%	0.0260	K_d = 4.2 ± 1.5 nM	36%	0.0265
Hill Equation	K_A = 37.4 ± 2.2 nM n = 1.45	5.9%	0.0265	K_A = 40.9 ± 1.9 nM n = 1.68	4.6%	0.0215
1:2 Stepwise	K_{d1} = 78 ± 14 nM K_{d2} = 36 ± 14 nM	18% 39%	0.0218	K_{d1} = 1300 ± 2100 nM K_{d2} = 1.3 ± 2.2 nM	160% 170%	0.0114
2 Independent	K_{d1} = 40 ± 370 nM K_{d2} = 50 ± 410 nM	860% 890%	0.0486	K_{d1} = 50 ± 16000 nM K_{d2} = 50 ± 16000 nM	32000% 32000%	0.0725